This is a postprint of an article published in
de Beer, D., Jerz, G., Joubert, E., Wray, V., Winterhalter, P.
Isolation of isomangiferin from honeybush (Cyclopia subternata) using high-speed counter-current chromatography and high-performance liquid chromatography
(2009) Journal of Chromatography A, 1216 (19), pp. 4282-4289.

Isolation of isomangiferin from honeybush (*Cyclopia subternata*) using high-speed counter-current chromatography and high performance liquid chromatography

Dalene de Beer [1,*], Gerold Jerz [2], Elizabeth Joubert [1,3], Victor Wray [4], Peter Winterhalter [2]

1 Post-Harvest and Wine Technology Division, ARC Infruitec-Nietvoorbij, Private Bag X5026, 7599 Stellenbosch, South Africa
2 Institute of Food Chemistry, Technical University of Braunschweig, Schleinitzstrasse 20, D-38106 Braunschweig, Germany
3 Department of Food Science, Stellenbosch University, Private Bag X1, Matieland, 7602 Stellenbosch, South Africa
4 Department of Structural Biology, Helmholtz Centre for Infection Research, Inhoffenstrasse 7, D-38124 Braunschweig, Germany

Abstract

Isomangiferin was isolated from *Cyclopia subternata* using a multi-step process including extraction, liquid-liquid partitioning, high-speed counter-current chromatography (HSCCC) and semi-preparative reversed-phase HPLC. Enrichment of phenolic compounds in a methanol extract of *Cyclopia subternata* leaves was conducted using liquid-liquid partitioning with ethyl acetate – methanol – water (1:1:2, v/v). The enriched fraction was further fractionated using HSCCC with a ternary solvent system consisting of *tert*-butyl methyl ether – *n*-butanol – acetonitrile – water (3:1:1:5, v/v). Isomangiferin was isolated by semi-preparative reversed-phase HPLC from a fraction containing mostly mangiferin and isomangiferin. The chemical structure of isomangiferin was confirmed by LC high-resolution electrospray ionization MS, as well as one and two dimensional NMR spectroscopy.

Keywords: Counter-current chromatography, *Cyclopia subternata*, Fabaceae, Isomangiferin, Mangiferin, Xanthones, NMR spectroscopy

[*] Corresponding author. Tel.: +27-21-8093449; fax: +27-21-8093430.
E-mail address: dbeerd@arc.agric.za (D. de Beer)

1. Introduction

Xanthones, constituents of many folk medicines, are a class of compounds known for a wide range of biological activities, which are associated with their tricyclic scaffold. The nature of their biological activities and their efficacy varies, depending on the nature and/or position of the different substituents [1]. Mangiferin (**1**) (Fig. 1), a mono-*C*-glucoside, is the major xanthone in an antioxidant product produced from mango bark (*Mangifera indica*) [2]. Another natural, and easily renewable source of mangiferin, is *Cyclopia* species (family: Fabaceae), which is endemic to the Cape Fynbos biome, a unique ecosystem in South Africa [3]. Commercial cultivation of *Cyclopia subternata* and *C. genistoides* has recently commenced. Investigation of the phenolic composition of *C. intermedia*, a species harvested in the wild, also revealed the presence of isomangiferin (**2**), a structural isomer of **1** differing only in the position of the *C*-glucosidic moiety [4]. HPLC-DAD (HPLC-diode array detection) analysis of a number of *Cyclopia* species showed that, in addition to **1**, they also contain **2**, albeit in smaller quantities [5,6]. *Cyclopia* species are used in oxidized ("fermented") form as an herbal tea and several *in vitro* and *in vivo* studies have demonstrated their antioxidant, antimutagenic and anticancer properties [3]. In view of the antioxidant and anti-inflammatory properties of **1** [1], the focus thus also falls on **2**. However, this compound is not commercially available for testing of its bioactivities. Relatively large quantities are required for testing in animal models. There also exists a need for the supply of reference material for HPLC-DAD analysis, routinely used in product development and the ARC's plant breeding and selection program, focussing on increasing the xanthone content of the plant material. Thus due to the preparative nature and scale-up possibilities of high-speed counter-current chromatography (HSCCC)[7], it could play an important role in isolation of large amounts of pure compounds needed for such research purposes. Previously **1** and **2** have been separated from *Iris florentina* (Asteraceae) [8] and *Senecio mikanioides* (Asteraceae) [9] using column chromatography with a polyamide stationary phase, while HSCCC isolation of **1** in the absence of **2** has been performed from extracts of *Anemarrhena asphodeloides* [10,11].

The aim of the study was to isolate **2** from *C. subternata* in order to unequivocally confirm its presence in this *Cyclopia* species using LC high-resolution electrospray ionization-MS (LC-HR-ESI-MS) with MS/MS fragmentation, as well as one and two dimensional NMR spectroscopy. The behaviour of other major compounds in the *C. subternata* extract during HSCCC fractionation in relation to **1** and **2** was also investigated. In addition, this investigation will provide the basis for future development of an isolation protocol of **2** from a *Cyclopia* spp. specifically selected for its high xanthone content.

2. Experimental

2.1. Reagents

Analytical grade organic solvents, acetonitrile, ethyl acetate, methanol, *n*-butanol, *iso*-propanol and *tert*-butyl methyl ether, from Merck (Darmstadt, Germany), dichloromethane and chloroform from SaarChem (Krugersdorp, South Africa), and Nanopure water (Barnstead, Dubuque, IA, USA) were used for sample preparation, HSCCC solvent selection experiments and HSCCC separation. For HPLC-DAD, HPLC Far UV gradient grade acetonitrile (BDH, VWR International, Poole, UK), formic acid (BDH, VWR International) and HPLC grade water were used. HPLC grade water was prepared by passing tap water sequentially through a Modulab Water Purification System (Continental Water Systems Corporation, San Antonio, TX, USA) containing in sequence carbon, reverse osmosis and deioniser cartridges and a Milli-Q water purifier (Millipore, Bedford, MA, USA). LC-HR-ESI-MS and –MS/MS analyses were performed using HPLC grade acetonitrile (Romil, Cambridge, UK), formic acid (Riedel-de Haën, Seelze, Germany) and Milli-Q purified water.

2.2. HPLC-DAD analysis

Reversed-phase HPLC-DAD analysis for quantification of the major phenolic compounds in the *C. subternata* extract and fractions was carried out on an Agilent 1200 series HPLC (Agilent Technologies, Waldbronn, Germany). The method of Joubert et al. [5] was slightly modified by changing to a Zorbax

Eclipse XDB column (150 x 4.6 mm; 5 µm particle size; Agilent Technologies) protected by a guard cartridge (12.5 x 4.6 mm) with the same stationary phase for improved peak shape and resolution of compounds. The aqueous mobile phase was also changed to 0.1% formic acid instead of 2% acetic acid to facilitate direct transfer to LC-HR-ESI-MS analysis, while acetonitrile was kept as the organic mobile phase. The flow rate and column temperature were 1.0 mL/min and 30 °C, respectively.

Solutions of *C. subternata* crude methanol extract, enriched fraction and HSCCC-fractions, dissolved in dimethylsulfoxide (DMSO), were filtered through 0.45 µm Millex-HV hydrophilic polyvinylidene fluoride (PVDF) syringe filters (Millipore) and automatically injected in duplicate at an appropriate volume. Authentic reference materials, i.e. compound **1** and hesperidin (**4**) from Sigma-Aldrich (St Louis, MO, USA), and eriocitrin (**3**) and luteolin (**5**) from Extrasynthese (Genay, France), were used for tentative peak identification according to retention times and UV-Vis spectra (Table 1). Compound structures are shown in Fig. 1. Quantification of peak area was performed according to a calibration series containing all standards injected at 10 µL and covering concentration ranges of 5 – 240, 2 – 100, 2 – 200 and 0.5 –20 mg/L for compounds **1**, **3**, **4** and **5**, respectively. Concentration ranges were selected based on expected concentration of compounds in samples. Four major unknown peaks were observed on the HPLC-DAD chromatogram of the crude methanol extract and enriched fraction and designated compounds **6-9**. Based on the UV-Vis spectra of the peaks (Table 1), compound **6** and **9** was classified as flavanones, compounds **8** as a flavone and compound **7** as a hydroxycinnamic acid. The xanthones (**1**, **2**), flavone (**5**), unknown hydroxycinnamic acid (**7**) and unknown flavone (**8**) were quantified at λ 320 nm and the known and unknown flavanones (**3, 4, 6, 9**) at λ 288 nm. Compound concentrations were expressed as g per 100 g dried extract or fraction. Compound **2**, differing from **1** only in the position of glycosylation and showing a similar UV-Vis spectra to **1** (Fig. 2), was quantified using **1** as standard with the assumption that their extinction coefficients should be similar. Compounds **7** and **8** were quantified as g luteolin equivalents per 100 g and compounds **6** and **9** as g hesperidin equivalents per 100 g due to similarities in their UV-Vis spectra.

2.3. LC-HR-ESI-MS and –MS/MS analysis

LC-HR-ESI-MS analysis of the crude methanol extract, HSCCC-fraction 9 and compounds **1** (Sigma-Aldrich) and **2** (isolated), was performed using a Waters API QTOF Ultima apparatus with a Waters UPLC system (Waters, Milford, MA, USA). Electrospray ionization in the positive and negative mode was carried out under the following conditions: desolvation temperature, 250 °C; nitrogen flow rate, 350 L/h; source temperature, 100 °C; capillary voltage, 3500 V; and cone voltage, 35 V. LC-HR-ESI-MS/MS was carried out at a collision energy of 20 V. Sodium formate was used for mass calibration to obtain an accurate mass determination of **2**. All other parameters were as for the HPLC-DAD analysis. The identity of peaks observed in the HPLC chromatograms was further confirmed by comparing their mass spectra with those of pure standard compounds.

*2.4. Isolation of **2***

2.4.1. Sample preparation

Plant material comprised dried, finely ground (Retsch mill, 1 mm sieve, Retsch GmbH, Haan, Germany) whole shoots (leaves and stems) of *C. subternata* harvested in April 2004 from a commercial plantation (Kanetberg Flora, Barrydale, Western Cape, South Africa). Plant material was first exhaustively extracted in a Soxhlet apparatus with dichloromethane to remove chlorophyll and related pigments. Thereafter, plant material (150 g) was extracted 3 times with 600 mL methanol in a batch-wise manner. The pooled methanol extracts were evaporated under vacuum (Büchi rotary evaporator, Büchi Labortechnik, Flawil, Switzerland) and freeze-dried (Edwards Modulyo freeze-drier, Edwards High Vacuum Ltd, Crowley, UK), yielding 19 g crude methanol extract. Enrichment of phenolic compounds in the extract was performed by partitioning a portion of the extract (9 g) in a mixture of ethyl acetate – methanol – water

(1:1:2, v/v; total volume = 1.2 L). The upper layer was removed and partitioning repeated with three 300 mL portions of ethyl acetate added to the lower layer. The pooled upper phases from each partitioning step, containing the enriched fraction (1.2 g) of medium polarity, was evaporated under vacuum (Büchi rotary evaporator) and freeze-dried (Christ freeze-drier, Martin Christ Gefriertrocknungsanlagen, Osterode am Harz, Germany) before HSCCC fractionation.

2.4.2. HSCCC solvent system selection

A range of solvent systems (Table 2) was tested for suitability to isolate compound **1** and **2** from *C. subternata* extracts. The enriched extract (2 – 5 mg) was dissolved in 500 µL each of the upper and lower phase of the pre-equilibrated solvent system and shaken in a glass vial. The settling time was recorded and 200 µL of each phase evaporated separately on a heating block at 50 ºC under a stream of nitrogen gas. The residues were redissolved in 200 µL 10% acetonitrile and analysed using HPLC-DAD (cf. 2.2.). The partition ratio for a given compound was calculated as:

K = [organic phase]/[aqueous phase].

2.4.3. HSCCC fractionation

The preparative HSCCC instrument used in the present study was a multilayer coil planet J-type centrifuge model CCC 1000 (Pharma-Tech Research, Baltimore, MD, USA), equipped with three preparative coils connected in series (polytetrafluorethylene (PTFE) tubing: 165 m x 2.6 mm i.d. with 876 mL theoretical total volume given by manufacturer, 850 mL measured total volume). The distance (revolution radius = R) of the holder axis of the coils to the central (solar) axis of the instrument was 7.5 cm. The inner β_r-value was measured to be 0.53 at the internal end of the coil and the outer β_r-value was 0.80 (equation: $\beta_r = r/R$; r is defined as the distance from the coil (planetary) axis to the nearest and farthest layer of the PTFE tubes wound on the coil system). The HSCCC system's direction of rotation determined the *head* locations at the periphery of the three coils.

HSCCC fractionation was performed with a two-phase solvent system composed of *tert*-butyl methyl ether – *n*-butanol – acetonitrile – water (3:1:1:5, v/v). After thoroughly equilibrating the solvent mixtures in a separatory funnel at room temperature, the two phases were separated shortly before use and degassed by ultrasonication. The upper organic phase was used as stationary phase and the lower aqueous phase as mobile phase in the *'head-to-tail'*-mode.

HSCCC fractionation was performed at ambient temperature with no temperature control during the separation. The multilayer coiled column was initially completely filled with the upper organic phase using a Biotronik BT 3020 HPLC pump (Jasco, Grossumstadt, Germany). The sample (550 mg) was dissolved in 10 mL each of upper and lower phase as suggested by Ito and Conway [12]. A precipitate (93 mg) formed which was filtered and kept as a separate fraction. The filtered sample solution was introduced into the separation column through a manual low-pressure sample injection valve (Rheodyne, Cotati, CA, USA) and a 25 mL loop without prior column equilibration. The lower phase was pumped at a flow rate of 3 mL/min in the *'head-to-tail'* direction after start of rotation at 850 rpm. The effluent stream from the *tail* outlet of the column was monitored by UV-absorbance at λ 280 nm using a Knauer K-2501 UV detector (Berlin, Germany) equipped with a preparative cell (0.5 mm path length) and collected into test tubes with a fraction collector (LKB SupeRac 2211, LKB, Bromma, Sweden) at 4 min intervals. After separation, the solvent in the coil was ejected with nitrogen gas to determine stationary phase retention (S_f), which was 58%. The ejected coil volume was also kept as an additional fraction. TLC analysis of all fractions was performed on silica 60 F_{254} plates (Merck) with chloroform – methanol – water – acetic acid (110:72:16:2, v/v) as eluant and visualization was with the universal spray reagent *p*-anisaldehyde – sulphuric acid – glacial acetic acid [13] followed by flash-heating at approximately 105ºC on a hot plate. Fractions were pooled according to similarities in observed TLC profiles.

2.4.4. Semi-preparative reversed-phase HPLC

Semi-preparative reversed-phase HPLC separation was performed on an Agilent 1200 series HPLC (Agilent Technologies) consisting of quaternary pump, autosampler, column thermostat, diode-array detector, fraction collector and Chemstation software for LC 3D systems (Rev. B.02.01). Separation took place on a Gemini C18 (150 x 10 mm; 5 µm particle size; 110 Å pore size) column, protected by a guard cartridge (10 x 10 mm) with the same stationary phase (Phenomenex, Santa Clara, CA, USA). The mobile phases, (A) 0.1% formic acid and (B) acetonitrile, were used in the following gradient: 0 – 8 min, 13% B; 8 – 10 min, 13 – 18% B; 10 – 15 min, 18 – 50% B; 15 – 17 min, 50 – 13% B; 17 – 27 min, 13% B. The flow rate and column temperature were maintained at 4.7 mL/min and 30 °C, respectively. HSCCC-fraction 9 (59 mg) was dissolved in DMSO and diluted with water (1:4) to ca. 6 mg/mL. The solution was filtered through 0.45 µm Millex-HV hydrophilic PVDF syringe filters (Millipore) and 100 µL injected repeatedly. The peak containing **2** were collected using automatic peak detection. The yield of compound **2** was 4.2 mg.

2.5. NMR analysis

^{1}H, ^{13}C, DEPT-135, and HMBC NMR spectra were recorded in DMSO-d_6 at 303 K on a Bruker AMX 300 spectrometer, and additionally at 353 K on a Bruker Avance ^{III} 600 MHz (Bruker Biospin, Rheinstetten, Germany) equipped with a cryo-probe head. Chemical shifts (δ) were reported in ppm relative to the residual solvent signals (δ_H 2.49 and δ_C 39.50 ppm) and coupling constants (*J*) in Hertz (Hz).

3. Results and discussion

3.1. Characterization of crude methanol extract

The crude methanol extract of *C. subternata* represents a complex mixture of compounds (Table 3). Among the constituents of the extract, the xanthone mono-*C*-glucoside structural isomers (**1, 2**), the flavanone rutinosides (**3-4**) and a flavone aglycon (**5**) have been previously isolated from *Cyclopia* spp. [4,14,15]. The unknown compounds **7**, **8** and **9** showed pseudo-molecular ions $[M+H]^+$ with *m/z* 615, 595 and 599, respectively, in the positive ionization mode (Table 4). No ionization in the positive mode was possible for compound **10**, but in the negative mode a pseudo-molecular ion $[M-H]^-$ with *m/z* 449 was observed. From the *m/z* of the pseudo-molecular ion and the fragment ions corresponding to the *m/z* of luteolin, compound **8** is presumably luteolin-7-*O*-rutinoside (scolymoside). Similarly, compound **6** is presumed to be an eriodictyol-glucoside from the *m/z* of the pseudo-molecular ion and the fragment corresponding to the *m/z* of eriodictyol. Scolymoside, eriodictyol-5-O-glucoside and eriodictyol-7-O-glucoside has been previously isolated from *C. subternata* [15]. Compounds **7** and **9** did not show LC-HR-ESI-MS and –MS/MS characteristics corresponding to compounds previously isolated from *C. subternata*.

*3.2. Isolation of isomangiferin (**2**)*

The crude methanol extract of *C. subternata* contains a relatively small amount of **2** (<1%) (Table 3; Fig. 2). In addition, most solvent systems in the polarity range of the sample, such as the ethyl acetate – *n*-butanol – water series and combinations of *tert*-butyl methyl ether – *n*-butanol – acetonitrile – water resulted in very long settling times (>60 s) in the presence of the crude extract (data not shown), which is not desirable for HSCCC separations. In order to enrich the extract and improve settling times by removing interfering compounds, liquid-liquid partitioning of the extract in ethyl acetate – methanol – water (1:1:2, v/v) was performed. This resulted in a fraction of medium polarity enriched in phenolic compounds, except for compounds **6**, **7** and **9**. (Table 3). The complexity of the extract decreased slightly as the polymeric compounds causing a broad baseline shift in the HPLC-DAD chromatograms were removed (Fig. 2). Compound **2** was enriched 4.5 times compared to the crude methanol extract. Several solvent systems were evaluated (Table 2) using the enriched fraction by determining the partition ratios (K) for the compounds. K values are usually a good predictor of the liquid-liquid distribution constant (K_D) in the HSCCC process. As

the most polar solvent system of the popular hexane – ethyl acetate – methanol – water solvent system family gave very low K values for **1** and **2**, more polar solvent system families consisting of ethyl acetate – *n*-butanol – water and *tert*-butyl methyl ether – *n*-butanol – acetonitrile – water were considered. Several of these gave acceptable K values for **1** and **2**, although α was too small (α of 1.5 or more theoretically needed for a good separation). Some solvent systems used in previous work on xanthone glycosides (chloroform – methanol – *iso*-propanol – water) [16] or specifically **1** (*n*-butanol – water; *n*-butanol – 1% acetic acid) [10,11] were also evaluated. The solvent system containing chloroform gave very low K values for **1** and **2** and was therefore not suitable. Both *n*-butanol – water (1:1, v/v) and *n*-butanol – 1% acetic acid (1:1, v/v) gave very similar results. *n*-Butanol – water (1:1, v/v) gave the best α value for **1** and **2**, but compounds **4** and **5** had very similar K values to that of **1** and **2**. Among the solvents systems tested, *tert*-butyl methyl ether – *n*-butanol – acetonitrile – water (3:1:1:5, v/v) was selected for HSCCC fractionation due to its excellent phase stability, short settling time in the presence of the sample (approx. 5 s) and K values for **1** and **2** close to 1, although compound **4** was predicted to co-elute with **1** and **2**. Despite the extensive search for a suitable solvent system spanning four solvent system families, none could be found to isolate **1** and **2** from *C. subternata* extracts without the need for additional semi-preparative HPLC.

Fractions from the HSCCC separation were pooled according to similarities of TLC profiles (Fig. 3). Some known and unknown compounds were quantified in the HSCCC fractions using HPLC-DAD (Table 3; Fig. 4). The precipitate formed during sample preparation for HSCCC contained mostly hesperidin (**4**) and scolymoside (**8**) with a small amount of eriocitrin (**3**). The HSCCC separation was done in the so-called *reversed phase* mode using the aqueous solvent layer as mobile phase, hence all relatively polar substances such as flavanone-rutinosides (**3** and **4**) eluted early (HSCCC-fraction 5 and 6), and the less polar xanthone mono-*C*-glucoside structural isomers later in HSCCC-fraction 9. Although hesperidin (**4**) appears to be relatively polar when comparing K values determined using the shake flask experiment, its solubility is low in water. HPLC analysis of HSCCC-fraction 5 detected a higher concentration of the more polar eriocitrin (**3**) than of hesperidin (**4**), and vice-versa fraction 6 contained more hesperidin (**4**). The additional 4'-methoxy group of hesperidin (**4**) is responsible for the slight decrease in its polarity compoared to eriocitrin (**3**). The less polar compounds luteolin (**5**) and **7** were only observed in the coil fraction. The elution order observed differed from that expected from the K values obtained in the shake-flask experiment. Eriocitrin (**3**) showed a higher K value than hesperidin (**4**) and scolymoside (**8**), but eluted before these two compounds. A similar effect has been observed previously [17]. A major difference between the two situations is that the sample solution as prepared for the HSCCC injection is much more concentrated than in the shake-flask experiment. Liquid-liquid distribution of compounds in a very concentrated solution may behave different than in less concentrated solutions due to interaction of compounds and matrix effects.

HSCCC-fraction 9 (64 mg; 12% yield of fraction from the extract subjected to HSCCC) (Fig. 3) contained **1** and **2** with only minor unknown impurities detected by HPLC-DAD (Fig. 5; Table 3), while major unknown ionizable impurities were detected by LC-HR-ESI-MS (Fig. 5). The HSCCC peak containing **1** and **2** had a partition ratio (K_D) of ca. 1.2 as calculated from the retention volume. The content of compound **2** in HSCCC-fraction 9 was enriched 5.5 times compared to the enriched fraction and 24.8 times compared to the crude methanol extract (Table 3). HSCCC was, therefore, a valuable methodology to pre-purify the two xanthone structural isomers from an enriched, though still quite complex fraction of *C. subternata* on a semi-preparative scale (550 mg sample loading). In this study, the sample loading was restricted due to available material, but it may be possible to increase the sample loading to obtain large scale preparative separation. The significant reduction in complexity of HSCCC-fraction 9 compared to the enriched fraction facilitated isolation of **2** (4.2 mg; 7% yield of **2** from sample subjected to semi-preparative HPLC) using semi-preparative HPLC (Fig. 6). Purity, calculated using HPLC-DAD, was 98 and 97% at 288 and 320 nm, respectively (Fig. 7). No impurities were detected using LC-HR-ESI-MS in the positive (Fig. 7) or negative (data not shown) ionization mode. The one dimensional NMR data (^{1}H, ^{13}C) also confirmed that impurities were below 2%.

*3.3. Elucidation of chemical structure of **2***

3.3.1. LC-HR-ESI-MS

LC-HR-ESI-MS in the positive ionization mode gave a molecular mass for the isolated **2** as $[M+H]^+$ of *m/z* 423.0936, which is within a 2.0 ppm range of the calculated mass, i.e. 423.0927. The LC-HR-ESI-MS/MS spectra of **1** and **2** obtained using positive ionization gave fragments similar to those obtained previously for **1** [18] (Table 3). Product ions consistent with the loss of H_2O (*m/z* 405), $2H_2O$ (*m/z* 387), as well as $2H_2O$ and HCHO (*m/z* 369), were observed using positive ionization. A product ion (*m/z* 303) representing a 120 amu loss from the molecular ion mass was observed, which has been reported to be typical for *C*-glycosides [19,20]. Other product ions (*m/z* 357, 327, 273) obtained in the positive mode could not be assigned. No product ion corresponding to the loss of a sugar moiety was observed as would be expected in the case of an *O*-glucoside. This result is typical of a *C*-glycoside. Interestingly, relative abundances for specific fragments were different for **2** compared to **1**, with the most abundant product ion for **2** and **1** being *m/z* 303 and *m/z* 273, respectively. This observation suggests that ESI-MS/MS intensities of generated fragment ions in the positive ionization mode might be an analytical tool for distinguishing different *C*-glucosidic substitution patterns in xanthones.

LC-HR-ESI-MS in the negative ionization mode gave fragments similar to those of **1** and **2** reported by Schieber et al. [20] (Table 3). Fewer product ions were observed in negative ionization mode compared to positive ionization. Two major product ions, representing a 120 (*m/z* 301) and 90 (*m/z* 331) amu loss from the molecular ion mass, were observed for both **1** and **2**. This pattern is typical of *C*-glycosides [19,20]. No major differences in product ion abundance were observed between **1** and **2**. From the results obtained it is clear that positive ionization is better than negative ionization for differentiating between **1** and **2**.

*3.3.2. One and two dimensional NMR of mangiferin (**1**) and isomangiferin (**2**)*

Mangiferin (**1**) (reference material cf. HPLC-DAD analysis) [21]: ^{13}C-NMR (75.5 MHz, d_6-DMSO): δ [ppm]: 179.6 (C-9), 163.7 (C-3), 161.7 (C-1), 156.1 (C-4a), 153.9 (C-6), 150.7 (C-10a), 143.6 (C-10), 111.7 (C-8a), 108.08/108.02 (C-2, signals of rotamers), 107.6 (C-8), 101.2 (C-9a), 93.3 (C-4), 81.4 (C-5'), 78.9 (C-3´), 73.0 (C-1´), 70.6 (C-4´), 70.2 (C-2´), 61.5 (C-6´).

Isomangiferin (**2**): ^{1}H-NMR (300 MHz, d_6-DMSO): δ[ppm]: 13.66 (1H, s, O<u>H</u> at C-1), 7.25 (1H, s, H-8), 6.55 (1H, s, H-5), 6.15 (1H, s, H-2), 4.80 (1H, d, *J* 7.0, H-1´); ^{13}C-NMR (75.5 MHz, d_6-DMSO): δ [ppm]: 178.4 (C-9), 162.8 (C-3), 161.4 (C-1), 158.2 (C-4a), 155.6 (C-6), 151.9 (C-10a), 144.8 (C-7), 108.9 (C-8a), 105.2 (C-8), 103.7 (C-4), 101.5 (C-9a), 101.3 (C-5), 97.1 (C-2), 81.3 (C-5´), 78.7 (C-3´), 73.3 (C-1´), 70.9 (C-4´), 70.7 (C-2´), 61.5 (C-6´).

The ^{1}H-NMR of **2** showed three typical singlet resonances of a xanthone partial structure with H-5 (δ 6.55 ppm), H-8 (δ7.25 ppm) and H-2 (δ6.15 ppm). The proton of the hydroxyl group at C-1 was strongly down-field at δ13.66 ppm due to hydrogen bonding with the carbonyl C-9. The anomeric proton of the *C*-glucosyl-unit was detected at δ4.80 ppm and the coupling constant indicated a β-glucopyranose configuration. For some protons of the *C*-glucose, signal broadening was observed caused by slow rotation about the *C*-glucose bond.

Nineteen carbon signals were detected in the ^{13}C-NMR spectrum of **2** representing the xanthone and the *C*-glucoside partial structure. A DEPT-135 experiment identified three CH-groups (C-5, δ101.3; C-8, δ 105.2; C-2, δ97.1 ppm) in the xanthone moiety and the anomeric C-1´ of the *C*-glucose at δ73.3 ppm. Our observed ^{13}C-NMR data of **2** were not in accord with the published reference data of **2** in d_6-DMSO reported by Fujita and Inoue [8]. There were significant differences in the range between $\Delta\delta$+2.5 and -2.5 ppm for the chemical shifts of C-4a (δ158.2 ppm), C-10a (δ108.9 ppm, C) and C-8 (δ105.2 ppm, CH). The published data [8] seemed to be similar to the data of **1** measured in d_6-DMSO [21]. We confirmed the ^{13}C-NMR data by a ^{13}C-NMR of authetic reference material (cf. HPLC DAD analysis) of mangiferin (**1**) and they were in accord with the published data of Frahm et al. [21]. Hence we conducted two dimensional NMR experiments (HMBC) to confirm the glucosidic linkage of the *C*-glucose at C-4 of the xanthone moiety and, therefore, the identity of **2** recovered from *C. subternata*.

Abundant $^{2,3}J$-CH long-range correlation signals corroborated the xanthone backbone with observed cross peaks from H-5 (δ 6.55) to C-6 (δ 158.2 ppm), C-7 (δ 144.8), C-10a (δ 151.9), C-8a (δ 108.9). A ^{4}J-CH long-range correlation was also detected to the carbonyl function C-9 (δ 178.38 ppm). For the same ring, the $^{2,3}J$-CH signals from H-8 (δ 7.25 ppm) to C-8a (δ 108.9), C-9 (δ 178.4), C-10a (δ 151.9), C-7 (δ 144.8 ppm), and the ^{4}J-CH to C-5 (δ 101.3) were observed (Fig. 1).

Signal broadening in the ^{1}H-NMR caused by slow rotation was partially overcome by measuring the HMBC at 353K (600 MHz). Interestingly, the HMBC at lower spectral dispersion at 300 MHz gave more intense $^{2,3}J$-CH correlation signals. In the case of the *C*-glucose unit, it solely allowed the detection of cross-peaks from H-1´ (δ 4.80 ppm) to C-4 (δ 103.7 ppm), and C-4a (δ 155.6 ppm) identifying the isomangiferin substitution with *C*-glucose at C-4. To the best of our knowledge, long-range CH-correlation data for isomangiferin (**2**) have not been published previously.

To summarize, critical resonances for identification of the positional isomers mangiferin (**1**), and isomangiferin (**2**) are two ^{13}C-NMR signals in the xanthone backbone: in the case of isomangiferin, C<u>H</u>-2 appeared as a very broad signal (δ 97.1 ppm), and C-4 attached to the *C*-glucose was detected at δ 103.7 ppm. Significantly in the case of **1**, the C<u>H</u>-4 appeared at a much higher field (δ 93.3 ppm), and C-2 appeared as two resonances at δ 108.08 and 108.02 ppm due to the existence of rotamers with slightly different δ-value chemical shifts.

4. Conclusions

The fast separation capabilities of counter-current chromatography, using high sample loads and also gentle isolation conditions, greatly improve the possible yields for recovery of unstable natural products. During our phytochemical investigation preparative high-speed counter-current chromatography (HSCCC) recovered a fraction highly enriched in the xanthone structural isomers, isomangiferin and mangiferin from a highly complex enriched fraction of *C. subternata* extract, for final isolation with semi-preparative HPLC. This is the first time that isomangiferin has been isolated from *C. subternata* and this work confirms its presence in this *Cyclopia* species. In terms of preparative purification of isomangiferin for use as a reference material, the procedure can be further optimised. Other *Cyclopia* species with higher isomangiferin contents will be investigated in future as starting material. Scale-up is also possible due to the nature of the HSCCC technique. Optimization of isomangiferin purification will be of great value in order to ascertain the various possible bioactivities of this compound.

Acknowledgements

Dr. Marietjie Stander from the Central Analytical Facility (Stellenbosch University, Stellenbosch, South Africa) is thanked for LC-HR-ESI-MS analyses. We are very grateful to Christel Kakoschke and Beate Jaschok-Kentner (Helmholtz Centre for Infection Research, Braunschweig, Germany) for technical assistance.

References

[1] M.M.M. Pinto, M.E. Sousa, M.S.J. Nascimento, Curr. Med. Chem. 12 (2005) 2517-2538.
[2] A.J. Núñez Sellés, H.T. Vélez Castro, J. Agüero-Agüero, J. González-González, F. Naddeo, F. De Simone, L. Rastrelli, J. Agric. Food Chem. 50 (2002) 762-766.
[3] E. Joubert, W.C.A. Gelderblom, A. Louw, D. de Beer, J. Ethnopharmacol. 119 (2008) 376-412.
[4] D. Ferreira, B.I. Kamara, E.V. Brandt, E. Joubert, J. Agric Food Chem. 46 (1998) 3406-3410
[5] E. Joubert, F. Otto, S. Grüner, B. Weinreich, Eur. Food Res. Technol. 216 (2003) 270-273.
[6] E. Joubert, E.S. Richards, J.D. van der Merwe, D. de Beer, M. Manley, W.C.A. Gelderblom, J. Agric. Food Chem. 56 (2008) 954-963.
[7] Y. Ito, J. Chromatogr. A 1065 (2005) 145-168.

370 [8] M. Fujita, T. Inoue, Chem. Pharm. Bull. 30 (1982) 2342-2348.
371 [9] S. Catalano, S. Luschi, G. Flamini, P.L. Cioni, E.M. Nieri, I. Morelli, Phytochem. 42 (1996) 1605-1607.
372 [10] Q. Sun, A. Sun, R. Liu, J. Chrom. A 1104 (2006) 69-74.
373 [11] T. Zhou, Z. Zhu, C. Wang, G. Fan, J. Peng, Y. Chai, Y. Wu, J. Pharm. Biomed. Anal. 44 (2007) 96-
374 100.
375 [12] Y. Ito, W.D. Conway, High-Speed Countercurrent Chromatography, Wiley, New York, 1996.
376 [13] E. Stahl, U. Kaltenbach, J. Chromatogr. 5 (1961) 351-355.
377 [14] B.I. Kamara, E.V. Brandt, D. Ferreira, E. Joubert, J. Agric. Food Chem. 51 (2003) 3874-3879.
378 [15] B.I. Kamara, D.J. Brand, E.V. Brandt, E. Joubert, J. Agric. Food Chem. 52 (2004) 5391-5395.
379 [16] H. Otsuka, Chem. Pharm. Bull. 47 (1999) 962-965.
380 [17] D. Gutzeit, P. Winterhalter, G. Jerz, J. Chrom. A 1172 (2007) 40-46.
381 [18] S. Suryawanshi, N. Mehrotra, R.K. Asthana, R.C. Gupta, Rapid Commun. Mass Spectrom. 20 (2006)
382 3761–3768.
383 [19] G. Rath, A. Touré, M. Nianga, J.-L. Wolfender, K. Hostettmann, Chromatographia 41 (1995) 332-342.
384 [20] A. Schieber, N. Berardini, R. Carle, J. Agric. Food Chem. 51 (2003) 5006-5011.
385 [21] A.W. Frahm, R.K. Chaudhuri, Tetrahedron Lett. 35 (1979) 2035-2038.
386

Figure captions

Fig. 1. Structures of mangiferin (**1**), isomangiferin with observed $^{2\text{-}4}J$-HC-long-range correlations from HMBC (**2**), eriocitrin (**3**), hesperidin (**4**) and luteolin (**5**).

Fig. 2. HPLC-DAD chromatogram of (A) methanol extract and (B) enriched fraction from *C. subternata* (inset: UV-Vis spectra of **1** and **2**). Column: Zorbax Eclipse XDB column (150×4.6 mm I.D., 5 µm); mobile phase: acetonitrile-formic acid (0.1%) (Acetonitrile: 0–6 min, 12%; 6–7 min, 12–18%; 7–14 min, 18–25%; 14–19 min, 25–40%; 19–24 min, 40–50%; 24–29 min, 50–12%; 29–40 min, 12%); flow-rate: 1.0 mL/min; detection wavelength: 288 nm.

Fig. 3. HSCCC chromatogram for fractionation of enriched *C. subternata* fraction (F9 = fraction containing **1** and **2**). Two-phase solvent system: *tert*-butyl methyl ether – *n*-butanol – acetonitrile – water (3:1:1:5, v/v); mobile phase: the lower aqueous phase; flow rate: 3.0 mL/min; revolution speed: 850 rpm; detection wavelength: 288 nm; sample size: 550 mg of enriched extract dissolved in 10 mL each of the lower and upper phases.

Fig. 4. HPLC-DAD chromatogram of HSCCC-fractions (each successive fraction was offset by 500 mAU on the y-axis for easy comparison). Conditions: cf. Fig. 2.

Fig. 5. LC-HR-ESI-MS total ion chromatogram (positive ionisation) for HSCCC-fraction 9. Column: Zorbax Eclipse XDB column (150×4.6 mm I.D., 5 µm); mobile phase: acetonitrile-formic acid (0.1%) (Acetonitrile: 0–6 min, 12%; 6–7 min, 12–18%; 7–14 min, 18–25%; 14–19 min, 25–40%; 19–24 min, 40–50%; 24–29 min, 50-12%; 29–40 min, 12%); flow-rate: 1.0 mL/min; detection wavelength: 288 nm.

Fig. 6. Chromatogram for semi-preparative isolation of isomangiferin (**2**) from HSCCC-fraction 9. Column: Phenomenex Gemini C18 column (150×10 mm I.D., 5 µm); mobile phase: acetonitrile-formic acid (0.1%) (Acetonitrile: 0–8 min, 13%; 8–10 min, 13–18%; 10–15 min, 18–50%; 15–17 min, 50–13%; 17–27 min, 13%); flow-rate: 1.0 mL/min; detection wavelength: 288 nm.

Fig. 7. (A) HPLC-DAD chromatogram, (B) LC-HR-ESI-MS total ion chromatogram (positive ionisation) of isomangiferin (**2**).Conditions: cf. Fig. 2; detection wavelength: 320 nm.

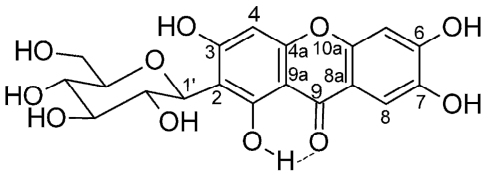

1

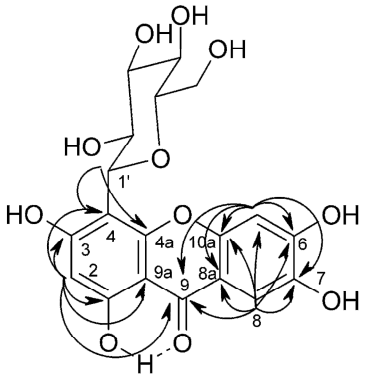

2

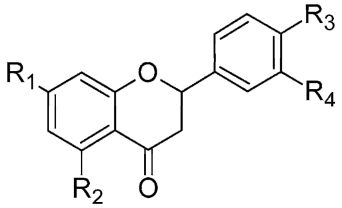

3: R_1 = O-rutinosyl; R_2, R_3, R_4 = OH

4: R_1 = *O*-rutinosyl; R_2, R_4 = OH; R_3 = OCH_3

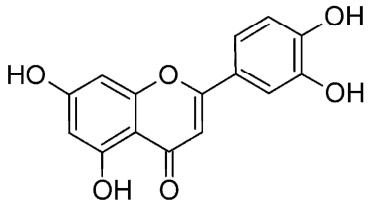

5

Figure 1

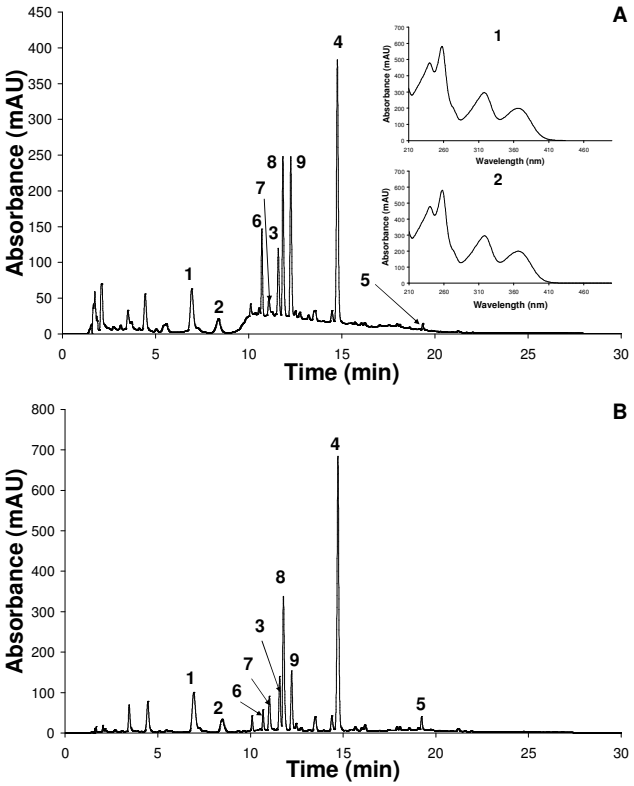
A
Absorbance (mAU)
Time (min)
Wavelength (nm)
1
2
3
4
5
6
7
8
9
B
Absorbance (mAU)
Time (min)
1
2
3
4
5
6
7
8
9

Figure 2

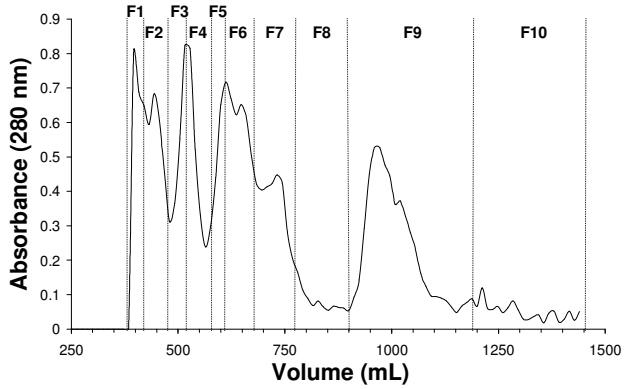
F1
F2
F3
F4
F5
F6
F7
F8
F9
F10
Absorbance (280 nm)
0.9
0.8
0.7
0.6
0.5
0.4
0.3
0.2
0.1
0
250
500
750
1000
1250
1500
Volume (mL)

Figure 3

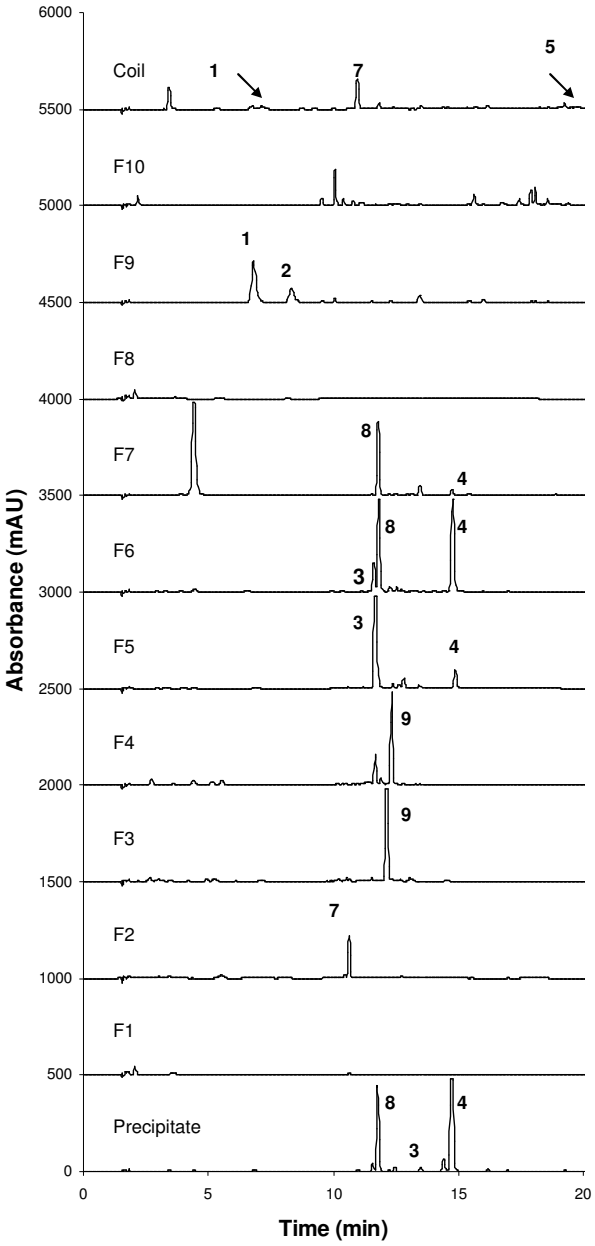
Coil
F10
F9
F8
F7
F6
F5
F4
F3
F2
F1
Precipitate
Absorbance (mAU)
Time (min)
6000
5500
5000
4500
4000
3500
3000
2500
2000
1500
1000
500
0
0
5
10
15
20

Figure 4

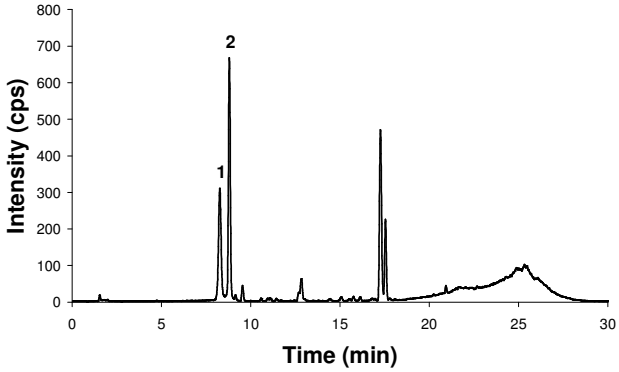

458
459 **Figure 5**

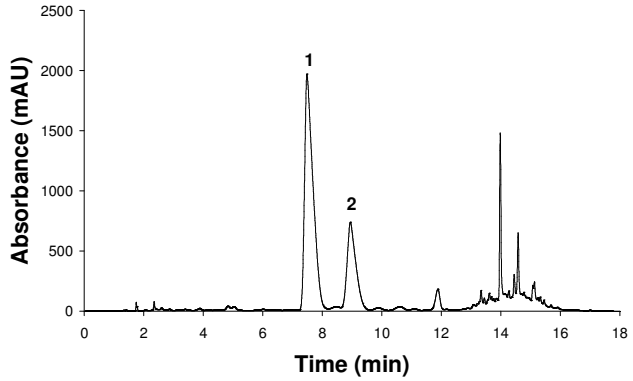

460
461 **Figure 6**

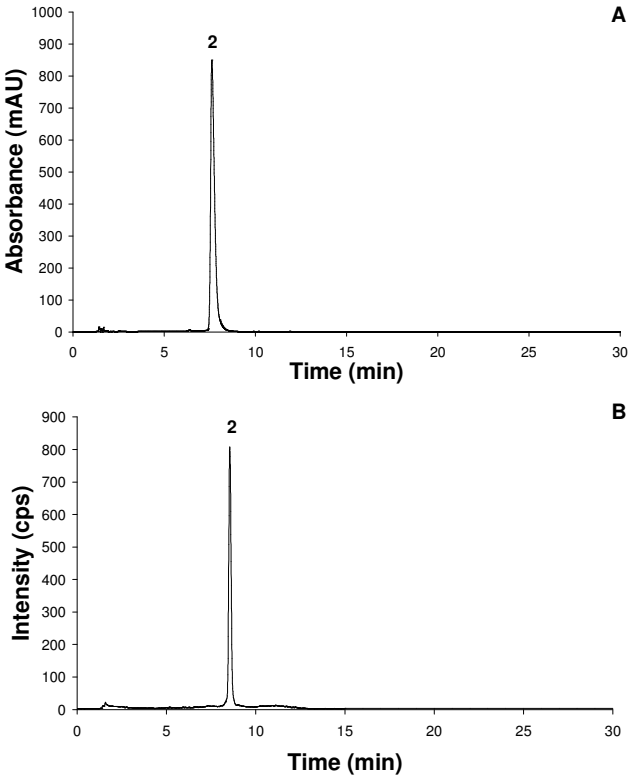

Figure 7